Enhancing infrared color reproducibility through multispectral image processing using RGB and three infrared channels

Motoshi Sobue[a,b,*] **Hiroshi Otake,**[b] **Hironari Takehara,**[a]
Makito Haruta,[a] **Hiroyuki Tashiro,**[a,c] **Kiyotaka Sasagawa,**[a]
and Jun Ohta[a]

[a]Nara Institute of Science and Technology, Division of Materials Science, Ikoma, Japan
[b]Nanolux Co. Ltd., Tokyo, Japan
[c]Kyushu University, Faculty of Medical Sciences, Fukuoka, Japan

Abstract. Various techniques for image color reproducibility under low-light conditions have been proposed, such as high sensitivity, a combination of visible (VIS) and infrared (IR) light, and coloring monochromatic images. However, when the illuminance falls below a certain level, color images cannot be obtained without prior color information. Previously, the exclusive use of IR without VIS illumination was proposed to achieve a pseudocolor image (basic IR color). It improved visibility compared with conventional monochrome images. However, there are cases, depending on the objects, when basic IR light cannot reproduce the correct color. An image processing method for enhancing color reproducibility is proposed, particularly for objects that are not suitable for the basic IR color (enhanced IR color). Moreover, we developed an algorithm to combine the advantages of both VIS and IR colors by utilizing signals of six wavelengths: three wavelengths each of VIS and IR. The proposed method includes an automatic transition between the optimal combination of VIS and IR colors when the illumination level changes, thus providing images with superior color reproducibility under various illumination levels compared with basic IR color. © *The Authors. Published by SPIE under a Creative Commons Attribution 4.0 International License. Distribution or reproduction of this work in whole or in part requires full attribution of the original publication, including its DOI.* [DOI: 10.1117/1.OE.61.6.063107]

1 Introduction

Various technologies and methods for improving image quality in low-light environments have been proposed. One of these approaches involves increasing the sensitivity of visible band (VIS) signals.[1–4] Another approach involves combining VIS and infrared (IR) light by obtaining luminance information from the sensor response of IR and synthesizing color information from the sensor response of VIS light so that color image representation can be used, even in dim environments.[5–13] However, neither of these methods can be used to obtain color information in the complete absence of VIS light. To solve this problem, the usual approach is color estimation of monochrome images. This is an image restoration technique based on the prior color information obtained by either one of the following options: (1) color specified by the user,[14–16] (2) arbitrary color images to estimate color of monochrome images,[17–19] or (3) machine learning using sample images.[20–22] The colorization technique, a method of obtaining a colorized IR image by using a color image as initial information, has also been proposed.[23–25] However, all these colorization techniques require to specify color information or to analyze many color images in advance.

It has been proposed to reproduce VIS color by the multispectral images in IR region.[26] Identifying spectral reflection in IR related to that in VIS, pseudocolor representation was

obtained only from the three IR response (basic IR color).[27,28] However, basic IR color was an approximation that could not achieve the high color reproducibility of VIS color.

In this study, we propose an image processing method for improving color reproducibility by effectively utilizing VIS light in addition to basic IR color in dim (enhanced IR color), particularly for the objects that are not suitable for basic IR color. The enhanced IR color is superior to basic IR color because it is comparable to basic IR color in dark and better in dim and bright illuminance conditions by utilizing VIS. Therefore, the enhanced IR color is a unique method providing favorable color reproducibility in dark, dim, and bright illuminance conditions without using prior color information. It should be noted that in this study, IR refers to near-IR, approximately in the range of 700 to 1000 nm. As for the illuminance level, the meanings of "bright," "dim," and "dark" are "enough VIS light," "low VIS light," and "absence of VIS light," respectively.

2 Basic IR Color

2.1 *Image Processing for Basic IR Color*

Basic IR color, which has been proposed previously, is a technique for colorizing an IR image close to the VIS color by performing color processing based on the weak relationship between the reflection characteristics of the objects in the VIS and IR range. Specifically, by attaching a correspondence between the three primary colors of VIS and the multiple wavelengths of IR, it is possible to estimate the VIS color based on the signal intensity of the multiple IR wavelengths and perform color representation.[29–31] Image processing methods for IR color are similar to those for VIS color, including white balance (WB), color correction (CC), and noise reduction (NR). An example of image processing for the basic IR color is shown in Fig. 1. It should be noted that image processing can be performed in various color spaces, such as RGB, YCbCr, and CIELab.

WB, CC, and NR are conventional image processing methods used for VIS as well. However, because the spectral reflections in the IR region are more gradual than those in the VIS region,[32] it is necessary to provide a specific adjustment in the image processing of IR color more than VIS color. The IR color-specific counterparts are as follows.

2.1.1 *White balance*

WB means here the global adjustment of the color intensities to make a white object appear white using IR illumination. Because the balance between IR wavelengths varies significantly depending on the light source irradiated on the objects and the sensitivity of the image sensor, the ratio of the IR signals from the imaging sensor can be largely diversified. Therefore, the WB gain must be applicable to a wider range of values (e.g., 0.125 to 8.0) than those for the VIS response. In addition, when a value of <1.0 is set for the WB gain, specific processing is required to avoid the so-called high-luminance coloring phenomenon, which causes unwanted coloring in the saturated portion of high luminance.

2.1.2 *Color correction*

Here, CC means a localized color adjustment allocating IR signals to VIS color. As for the characteristics of the materials used as objects, the spectral characteristics in the IR wavelength
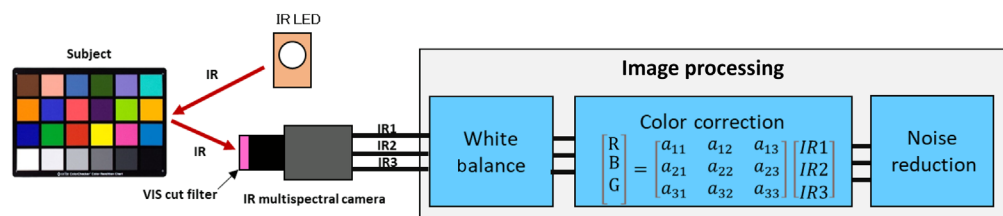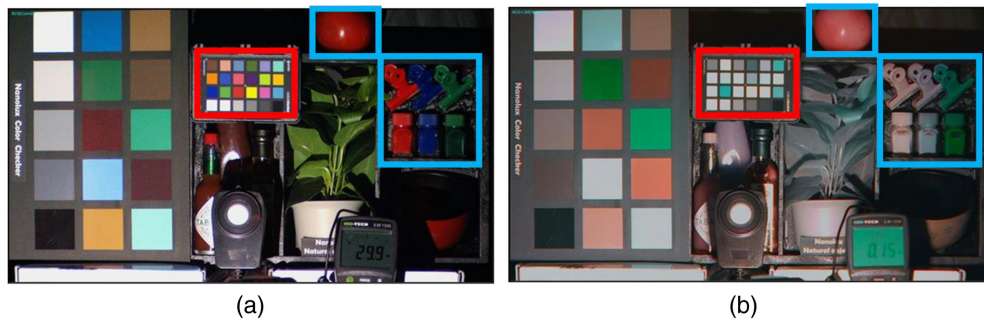

Fig. 1 Example of IR color camera and image processing flow.

(a)   (b)

Fig. 2 Sample images of VIS and basic IR color: (a) VIS color in bright illuminance (30 lux) and (b) IR color in dark illuminance (No VIS used).

region are generally less sensitive than those in the VIS wavelength region, and the relative changes between wavelengths are more gradual. To visualize such feature representation, it is necessary to provide relatively strong correction effect, such as a variable range of ± 4.0 for the RGB 3×3 matrix coefficients. The colors are adjusted through matrix correction to the approximate VIS color.

2.1.3 *Noise reduction*

Owing to the strong correction gain, the NR function plays a crucial role along with the CC function. Maintaining minimum noise while optimizing image quality, including sharpness and edge expression, is essential. In this system, two types of filters, space NR (Gaussian type smoothing filter) and time axis NR (frame addition) are combined especially in low IR illumination where the noise level is high. The purpose of basic IR color is providing color information and it has a trade-off relationship with NR; therefore, an appropriate balance should be set between both.

2.2 *Example of VIS and Basic IR Color*

Figure 2 shows an example of the VIS and basic IR color. The objects surrounded by blue frames (tomatoes, ink bottles, and paper clips) reproduce color relatively well, whereas the Macbeth chart surrounded by red frames shows low color reproducibility, thereby suggesting that the accuracy of color reproducibility varies depending on the objects.

3 Enhanced IR Color

In this section, we describe an imaging process to enhance IR color utilizing RGB-3NIR six-channel multispectral signals. Although basic IR color uses only IR light assuming complete darkness, in practical applications, such as surveillance, it is rare that there is no VIS light. There are many dim situations where there is a small amount of VIS light. In such cases, instead of providing basic IR color by cutting off all VIS light, we examined a method for improving color reproducibility by effectively utilizing weak VIS signals.

The camera system used in this study is illustrated in Fig. 3. The multispectral camera (NLX-PH001-C) was selected because it is designed to provide VIS and basic IR color. The camera has 3CMOS with a spectrum prism as shown in the transmittance characteristics in Fig. 3. Each CMOS detects different VIS and IR bands: the first CMOS for R and IR1 (810 nm), the second CMOS for B and IR2 (870 nm), and the third CMOS for G and IR3 (940 nm). The camera works as a VIS camera when attaching an IR cut-filter and as a basic IR color camera with a VIS cut-filter. In this exercise, two of these cameras were used because one camera cannot provide VIS and IR six-channel multispectral signals. One (CAM1) is equipped with an IR-cut filter to transmit only R, B, and G. The other without a filter (CAM2) transmits R and IR1, B and IR2, G and IR3. The angles and distance of both cameras are adjusted with using calibration software to
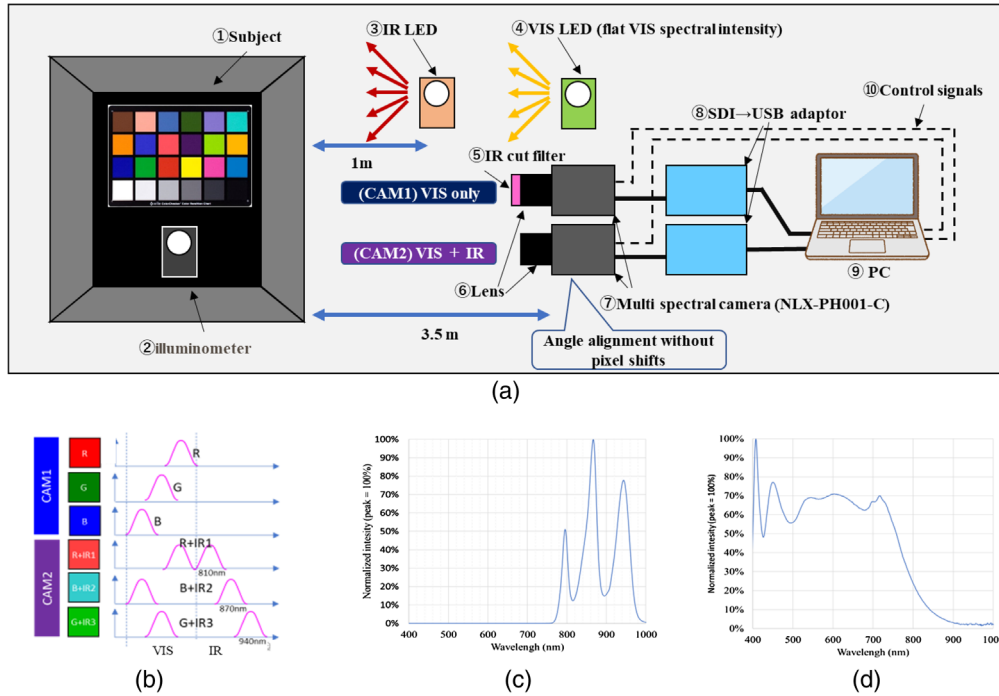
Fig. 3 Evaluation system of the enhanced IR color camera: (a) the total system, (b) schematic channel responses for CAM1 and CAM2, (c) normalized spectral intensity of IR illumination (Nanolux Co. Ltd., multi-IR illuminator), and (d) that of VIS illumination (CCS Inc., XX-SC28FS55-P1).

avoid pixel shifts. There are two illuminators for the VIS and IR. The VIS illuminator is variable for adjusting the darkness. The IR illuminator is constant and irradiates IR1, IR2, and IR3 light to the target.

The image processing algorithm for enhanced IR color is shown in Fig. 4. Three unique issues of enhanced IR color must be considered: The first issue is the difference in the spectrum characteristics in the VIS and IR ranges; an optimal image cannot be obtained by simply summing the VIS and IR colors but has to be processed in VIS and IR ranges separately. The second issue is the dynamic transition of the optimal composite ratio of VIS and IR images based on illuminance level; for higher illuminance level, VIS is more reliable than IR color. Therefore, the optimal composite ratio needs to be calculated in the algorithm seamlessly and automatically. The third issue is the relatively weak spectral reflections in the IR region compared with those in
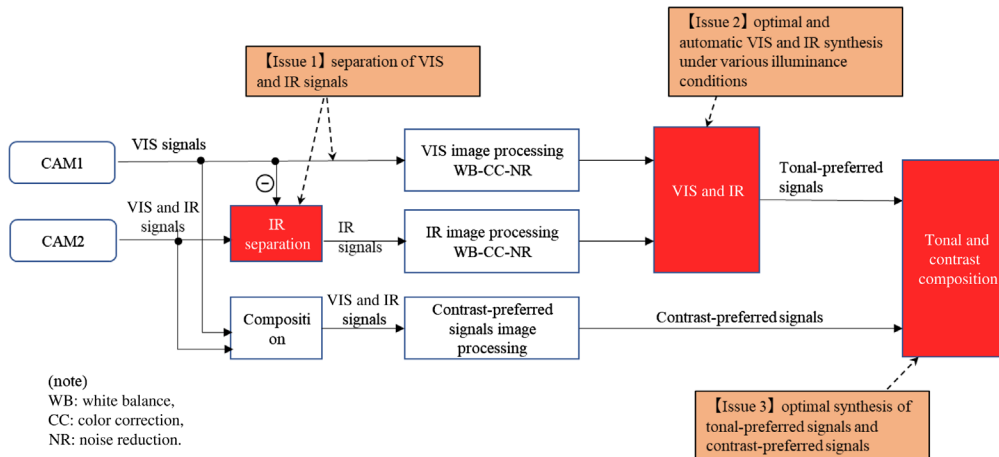
Fig. 4 Algorithm for enhanced IR color and three main issues.

the VIS region. Therefore, a strong parameter is required in WB and CC in IR image processing as described in Sec. 2.1. To compensate the noise caused by the strong parameters, a spatial quality signal such as SN (contrast-preferred signal) is separately calculated and added to the signals generated with emphasis on color expression such as hue and Chroma (tonal-preferred signal) in VIS and IR.

3.1 Solution to Issue 1: Difference in Spectrum Characteristics in VIS and IR Ranges

Because simply summing the VIS and IR colors will not produce an appropriate color, image processing is required in VIS and IR separately. Thus, three VIS and three IR signals are needed. In the camera system shown in Fig. 3, VIS signals are acquired from CAM1, whereas the IR signals require calculation based on the difference between CAM2 and CAM1. Considering that the IR-cut filter on CAM1 is not fully transmitted, the specific formula for extracting IR signals is expressed as follows:

$$R_i = \frac{g_i}{g_n} R_n - \frac{g_i}{g_v t_R} R_v, \tag{1}$$

$$G_i = \frac{g_i}{g_n} G_n - \frac{g_i}{g_v t_G} G_v, \tag{2}$$

$$B_i = \frac{g_i}{g_n} B_n - \frac{g_i}{g_v t_B} B_v, \tag{3}$$

where R_v, G_v, and B_v are the VIS signal from CAM1 after preprocessing, including black correction, defect correction, and distortion correction, R_n, G_n, and B_n are the VIS and IR signals from CAM2 after preprocessing, including black correction, defect correction, and distortion correction, R_i, G_i, and B_i are the IR signals (calculated), g_v is the gain values applied to CAM1 sensors, g_n is the gain values applied to CAM2 sensors, g_i is the gain value to be applied to the IR signal, t_R, t_G, and t_B are the rate at which VIS signals are attenuated by the installation of the IR-cut filter.

3.2 Solution to Issue 2: Optimal and Automatic VIS and IR Composition Under Various Illuminance Levels

As the lighting environment changes, the optimal composition ratio of VIS and IR colors changes as well. It is necessary to automatically transit the optimal composition of the VIS and IR colors according to the external lighting environment. Although linking parameters by installing a separate illuminance sensor could be considered, the price and complexity of such a method would be impractical. Therefore, we develop a method for setting the optimal composition ratio without an additional sensor by referring to the auto gain value from the auto exposure (AE) function of the camera.

The basic idea of the method is that (1) as the auto gain value for VIS decreases, the composition ratio of VIS decreases and that of IR increases, and (2) as the auto gain value for IR decreases, the composition ratio of IR decreases as well.

The composition is performed on the signals after WB correction, CC, and gamma conversion, as shown in the "VIS and IR composition" presented in Fig. 4. The composition formula is a simple weighted sum operation, which is expressed as follows:

$$\begin{bmatrix} Y \\ C_{bl} \\ C_{rl} \end{bmatrix} = \begin{bmatrix} w_{vY} \ Y'_v \\ w_{vC} \ C'_{bv} \\ w_{vC} \ C'_{rv} \end{bmatrix} + \begin{bmatrix} w_{iY} \ Y'_i \\ w_{iC} \ C'_{bi} \\ w_{iC} \ C'_{ri} \end{bmatrix}, \tag{4}$$

where $Y_{v'}$, $C_{bv'}$, and $C_{rv'}$ are the color reproducibility signal after development from VIS response. $Y_{i'}$, $C_{bi'}$, and $C_{ri'}$ are the color representation signal after development from IR response. w_{vY} is the weight coefficient for luminance signal $Y_{v'}$ after development from VIS

response. w_{vC} is the weight coefficient for chromaticity signals $C_{bv'}$ and $C_{rv'}$ after development from VIS response. w_{iY} is the weight coefficient for luminance signal $Y_{i'}$ after development from IR response. w_{iC} is the weight factors for chromaticity signals $C_{bi'}$ and $C_{ri'}$ after development from IR response.

At next, the weight coefficients for the VIS light response, w_{vY} and w_{vC}, are calculated using the gain values for the VIS response

$$w_{vY} = w_{vC} = F_{DQv}(D_{av}), \qquad (5)$$

where D_{av} is the auto gain value for VIS response (dB). D_{ai} is the auto gain value for IR response (dB). F_{DQv} is the evaluation function of VIS image quality through VIS response gain.

As the auto gain value of the VIS light decreases, the ratio of VIS light should decrease as well.

Finally, the weight coefficients w_{iY} and w_{iC} for the IR response are calculated using the gain values for the VIS and IR responses

$$w_{iY} = F_{DvSY}(D_{av}) \times F_{DQi}(D_{ai}), \qquad (6)$$

$$w_{iC} = F_{DvSC}(D_{av}) \times F_{DQi}(D_{ai}), \qquad (7)$$

where F_{DvSY} and F_{DvSC} are the evaluation function of each signal complement intensity through VIS response gain, F_{DQi} is the evaluation function of IR response image quality through IR light response gain.

F_{DvSY} and F_{DvSC} represent the strength of the IR signal that is allowed to complement the signal obtained from the VIS response when it decreases, and they should be set such that they increase as the gain value for the VIS response decreases.

Figure 5(a) shows an example of the evaluation function. Complementation through the IR signal is set to start at a slightly higher gain, which is intended to keep the VIS color as intact as possible. If the color approximation of the IR color is higher, complementation through the IR signal can be set to start at a lower gain.

F_{DQi} is set to reduce the weighting of the IR color when the signal from the IR light response decreases, thereby indicating that the IR color is no longer reliable, as shown in Fig. 5(b).

3.3 Solution to Issue 3: Optimal Composition of Tonal- and Contrast-Preferred Signals

The final image is constructed by applying separately generated contrast- and tonal-preferred signals obtained by the method explained in Sec. 3.2.

The advantage of the contrast-preferred signal is to combine the full signals from the two cameras. Figure 6 shows the detailed processing configuration for combining the tonal- and contrast-preferred signals. As shown in Fig. 6, the contrast-preferred signal is used as the base signal. The difference between the tonal- and contrast-preferred signals is used as an additional
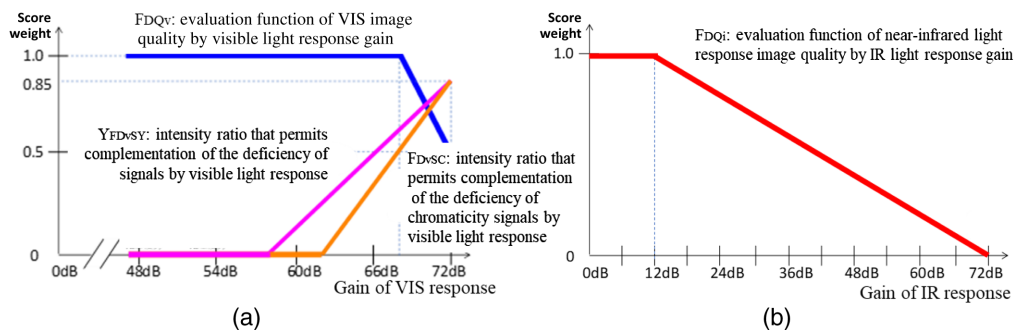
Fig. 5 Example of evaluation functions for color composition: (a) evaluation function from VIS response and (b) evaluation function from IR response.
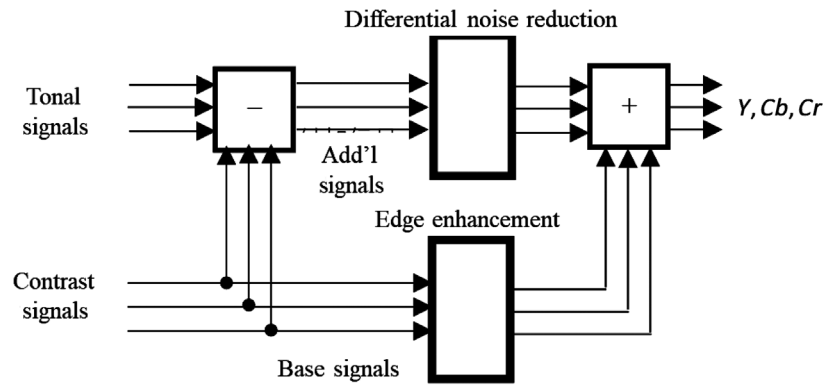
Fig. 6 Detailed processing configuration for tonal- and contrast-preferred signal composition.
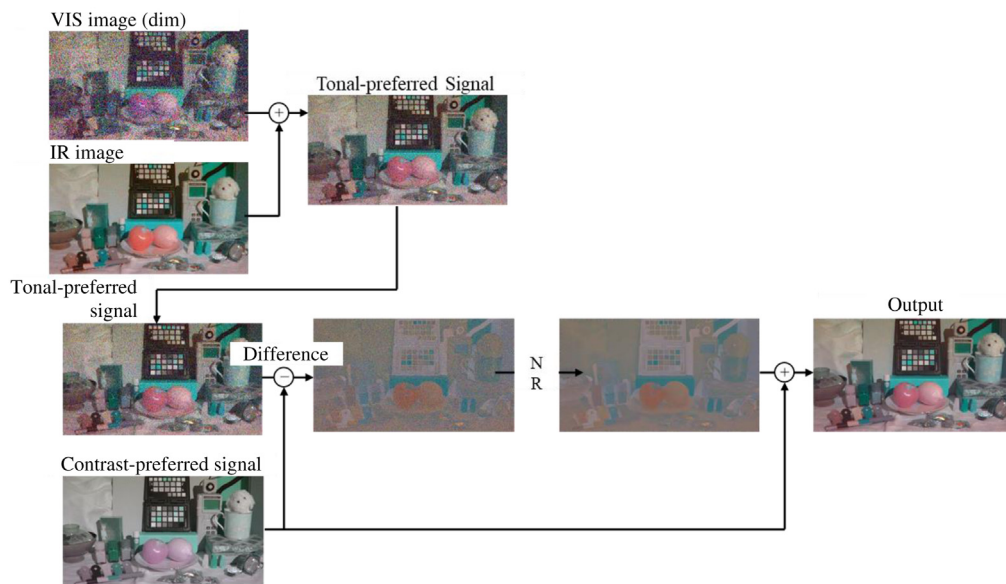
Fig. 7 Example of images in the tonal- and contrast-preferred composition process.

signal to ensure the quality of chromatic expression that is finally added for output. The spatial filter for NR processing applied to the tonal-preferred signal or additional signal is an edge-preserving low-pass filter that reduces the high-frequency component caused by noise, but it retains the edge components as much as possible. Finally, the two signal spatial filter was used as an effective process for achieving differential NR.

The image processing for the tonal- and contrast-preferred signal composition process is shown in Fig. 7.

4 Experimental Evaluations

The images obtained using the enhanced IR color system in bright (30 lux), dim (0.7 lux), and dark (0.15 lux) illuminance are compared with basic IR and VIS in Fig. 8. Enhanced IR color provides better color reproducibility of the Macbeth chart (see the red boxes) in dim light than basic IR color while achieving color reproducibility comparable to basis IR in dark and VIS in bright illuminance.

Figure 9 shows the quantitative evaluation of color reproducibility of the Macbeth chart. We select 12 colors in the second and third rows from the top of the standard, where it was difficult to reproduce the colors using basic IR color. Because the main purpose of the study is to reproduce VIS color using the multispectral signals, the chromatic variance (ΔC_{ab}) is measured, using the

Fig. 8 Enhanced IR color, basic IR color, and VIS color by illumination level.
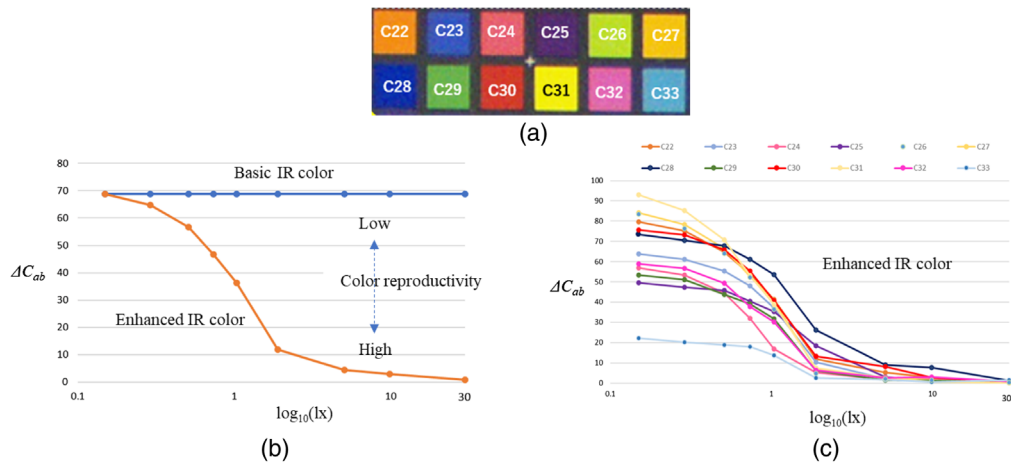

Fig. 9 Chroma reproducibility evaluation of basic IR color and enhanced IR color of Macbeth chart: (a) 12 colors of Macbeth chart used for the evaluation, (b) distances from the correct color (VIS color in bright) on *ab*-space on average of 12 colors, and (c) those of each color.

distance from the correct color of VIS in bright (30 lx) illuminance in the $a - b$ dimension of the CIELab color space[33]

$$\Delta C_{ab} = \{\Delta a^2 + \Delta b^2\}^{1/2}, \tag{8}$$

where Δa and Δb are the difference of a and b coordinates between enhanced IR color and basic IR color on the CIELab space.

The shorter the distance, the more reproducible the chroma. Because basic IR color does not utilize VIS light, there is always a large discrepancy from the VIS color regardless of the illuminance. In contrast, enhanced IR color provides more reproducible colors than basic IR color, not only in bright but also in dim light.

To verify the reproducibility of other objects, the same analysis was performed on the three ink bottles (see the dotted blue boxes in Fig. 8), which achieved relatively good color
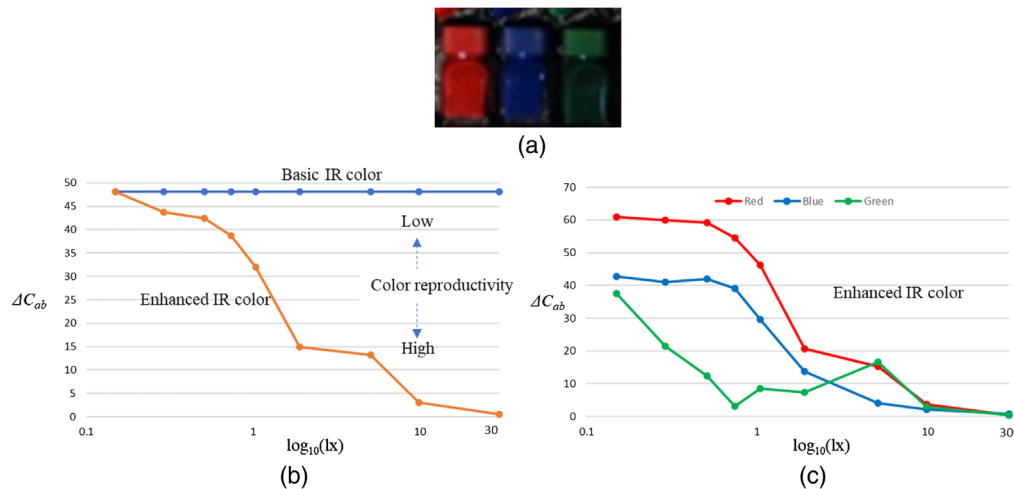
Fig. 10 Chroma reproducibility evaluation of basic IR color and enhanced IR color of ink bottles: (a) three colors of ink bottles used for the evaluation, (b) distances from the correct color (VIS color in bright) on *ab*-space on average of three colors, and (c) those of each color.

reproducibility using basic IR color (Fig. 10). Comparing the color reproducibility of basic IR color with the Macbeth chart presented in Fig. 9, the ink bottles indicate slightly better color reproducibility (66 vs. 47). Comparing the basic IR color with the enhanced IR color, the latter is superior on average at all illumination levels for all three colors, although there are cases where the color expression is better in darker illuminance, e.g., the green bottle under 0.7 to 5.1 1ux. Thus, it was determined that enhanced IR color can achieve more reproducible colors than basic IR color, particularly for objects with poor color reproducibility.

5 Conclusion

We proposed an image processing method for improving color reproducibility compared with that of basic IR. By utilizing a total of six channels (three VIS and IR wavelengths each), we confirmed that the color reproducibility of enhanced IR color exceeded that of basic IR color under all light conditions. We also proposed an algorithm that takes advantage of both VIS and IR colors to automatically transition the optimal composition of VIS and IR colors using auto-gain values that can be easily obtained from an ordinary camera. We confirmed the superiority of enhanced IR color to basic IR color for various objects, particularly for objects with poor color reproducibility in basic IR color.

References

1. A. Artusi et al., "High dynamic range imaging technology [Lecture notes]," *IEEE Signal Process. Mag.* **34**(5), 165–172 (2017).
2. M. Kubota et al., "Ultrahigh-sensitivity new super-HARP camera," *IEEE Trans. Broadcast.* **42**(3), 251–258 (1996).
3. Canon Inc., "Canon develops SPAD sensor with world-highest 3.2-megapixel count, innovates with low-light imaging camera that realizes high color reproduction even in dark environments," (2021).
4. M. Furuta et al., "A high-speed, high-sensitivity digital CMOS image sensor with a global shutter and 12-bit column-parallel cyclic A/D converters," *IEEE J. Solid-State Circuits* **42**(4), 766–774 (2007).
5. S. Sekiguchi and M. Yamamoto, "Near-infrared image colorization by convolutional neural network with perceptual loss," in *IEEE 9th Global Conf. Consum. Electron. GCCE)*, IEEE, pp. 88–89 (2020).

6. C. Williams et al., "Grayscale-to-color: scalable fabrication of custom multispectral filter arrays," *ACS Photonics* **6**(12), 3132–3141 (2019).

7. N. Hagen and M. W. Kudenov, "Review of snapshot spectral imaging technologies," *Opt. Eng.* **52**(9), 090901 (2013).

8. H.-J. Kwon and S.-H. Lee, "Visible and near-infrared image acquisition and fusion for night surveillance," *Chemosensors* **9**(4), 75 (2021).

9. H. Su, C. Jung, and L. Yu, "Multi-spectral fusion and denoising of color and near-infrared images using multi-scale wavelet analysis," *Sensors* **21**(11), 3610 (2021).

10. H. Yamashita, D. Sugimura, and T. Hamamoto, "Enhancing low-light color images using an RGB-NIR single sensor," in *Vis. Commun. and Image Process. (VCIP)*, pp. 1–4, IEEE (2015).

11. T. Honda, D. Sugimura, and T. Hamamoto, "Multi-frame RGB/NIR imaging for low-light color image super-resolution," *IEEE Trans. Comput. Imaging* **6**(XX), 248–262 (2020).

12. J. M. Amigo, H. Babamoradi, and S. Elcoroaristizabal, "Hyperspectral image analysis. A tutorial," *Anal. Chim. Acta* **896**, 34–51 (2015).

13. Z. Chen, X. Wang, and R. Liang, "RGB-NIR multispectral camera," *Opt. Express* **22**(5), 4985 (2014).

14. A. Levin, D. Lischinski, and Y. Weiss, "Colorization using optimization," *ACM Trans. Graphics* **23**(3), 689–694 (2004).

15. L. Yatziv and G. Sapiro, "Fast image and video colorization using chrominance blending," *IEEE Trans. Image Process.* **15**(5), 1120–1129 (2006).

16. J. Mairal, M. Elad, and G. Sapiro, "Sparse representation for color image restoration," *IEEE Trans. Image Process.* **17**(1), 53–69 (2008).

17. E. Reinhard et al., "Color transfer between images," *IEEE Comput. Graphics Appl.* **21**(4), 34–41 (2001).

18. T. Welsh, M. Ashikhmin, and K. Mueller, "Transferring color to greyscale images," in *Proc. 29th Annu. Conf. Comput. Graphics and Interact. Tech. - SIGGRAPH '02*, ACM Press, New York, p. 277 (2002).

19. R. K. Gupta et al., "Image colorization using similar images," in *Proc. 20th ACM Int. Conf. Multimedia – MM '12*, ACM Press, New York, p. 369 (2012).

20. Z. Cheng, Q. Yang, and B. Sheng, "Deep colorization," in *IEEE Int. Conf. Comput. Vision (ICCV)*, IEEE, pp. 415–423 (2015).

21. S. Iizuka, E. Simo-Serra, and H. Ishikawa, "Let there be color!" *ACM Trans. Graphics* **35**(4), 1–11 (2016).

22. R. Zhang, P. Isola, and A. A. Efros, "Colorful image colorization," *Lect. Notes Comput. Sci.* **9907**, 649–666 (2016).

23. T. Hamam, Y. Dordek, and D. Cohen, "Single-band infrared texture-based image colorization," in *IEEE 27th Convention of Electr. and Electron. Eng. in Israel*, IEEE, pp. 1–5 (2012).

24. M. Limmer and H. P. A. Lensch, "Infrared colorization using deep convolutional neural networks," in *15th IEEE Int. Conf. Mach. Learn. and Appl. (ICMLA)*, IEEE, pp. 61–68 (2016).

25. P. L. Suárez, A. D. Sappa, and B. X. Vintimilla, "Learning to colorize infrared images," in *Advances in Intelligent Systems and Computing*, F. D. Prieta et al., Eds., Springer Verlag, pp. 164–172 (2017).

26. M. Vilaseca, J. Pujol, and F. M. Martínez-Verdú, "Color visualization system for near-infrared multispectral images advanced digital reproduction of visual gonio-appearance of objects (ADIREVGAO) View project Metallic Coatings View project," *J. Imaging Sci. Technol.* **49**(3) (2005).

27. H. Takehara et al., "Multispectral near-infrared imaging technologies for nonmydriatic fundus camera," in *IEEE Biomed. Circuits and Syst. Conf. (BioCAS)*, IEEE, pp. 1–4 (2019).

28. National Institute of Advanced Industrial Science and Technology (Japan), "Development of high-definition infrared color night-vision imaging technology," 2013, https://www.aist.go.jp/aist_e/list/latest_research/2013/20130201/20130201.html (accessed 13 Jan. 2022).

29. Y. Nagamune, "Imagine capturing device and image capturing method," US Patent 8854472 (2014).

30. Y. Nagamune, "Image capturing device and image capturing method," US Patent 8836795 (2014).
31. H. Sumi et al., "Next-generation fundus camera with full color image acquisition in 0-lx visible light by 1.12-micron square pixel, 4K, 30-fps BSI CMOS image sensor with advanced NIR multi-spectral imaging system," in *IEEE Symp. VLSI Technol.*, pp. 163–164 (2018).
32. Y. Asano et al., "Shape from water: bispectral light absorption for depth recovery," *Lect. Notes Comput. Sci.* **9914**, 635–649 (2016).
33. R. Berns, *Billmeyer and Saltzman's Principles of Color Technology*, pp. 107–130, Wiley & Sons, Inc. (2000).

Motoshi Sobue received his MS degree in engineering from Waseda University, Japan, in 1989 and his MA degree in economics from Duke University, USA, in 1996. He worked for Bank of Japan, Intel, Dell, and BAT. In 2021, he joined the Graduate School of Material Science, Nara Institute of Science and Technology (NAIST), Nara, Japan, as a PhD candidate. He has his own business as a CEO of Nanolux Co. Ltd.

Hiroshi Ohtake graduated from the Tokyo Kogakuin College of Technology, Tokyo, Japan, in 1982. In 1982, he joined the Japan Broadcasting Corporation (NHK), Tokyo. Since then, he has been engaged in the development of advanced image sensors in the Science and Technology Research Laboratories. Since August 2020, he has been with Nanolux corporation and research of multispectral image sensors. He is a fellow member of the Institute of Image Information and Television Engineers.

Hironari Takehara received his ME degree in applied chemistry from Kansai University, Osaka, Japan, in 1986, and a PhD degree in materials science from Nara Institute of Science and Technology (NAIST), Nara, Japan, in 2015, respectively. From 1986 to 2012, he was a semiconductor process engineer at Panasonic Corporation, Kyoto, Japan. In 2015 and 2019, he joined NAIST as a postdoctoral fellow and assistant professor, respectively. His current research interests involve CMOS image sensors and bioimaging.

Makito Haruta received his MS degree in biological science and his Dr. Eng degree in material science from the Nara Institute of Science and Technology (NAIST), Nara, Japan, in 2011 and 2014, respectively. He joined NAIST in 2016 as an assistant professor. In 2019, he joined the Graduate School of Science and Technology, NAIST, as an assistant professor. His research interests include brain imaging devices for understanding brain functions related to animal behaviors.

Hiroyuki Tashiro received his ME degree from Toyohashi University of Technology in 1996. He received his PhD from Nara Institute of Science and Technology (NAIST) in 2017. In 1998, he joined Nidek Co., Ltd., working on the R&D of ophthalmic surgical systems and retinal prostheses. He has been an assistant professor at Kyushu University since 2014 and an associate professor at NAIST since 2019. His current research interests include artificial vision systems and neural interface.

Kiyotaka Sasagawa received his BS degree from Kyoto University in 1999 and his ME and PhD degrees in materials science from NAIST, Japan, in 2001 and 2004, respectively. Then, he was a researcher with the National Institute of Information and Communications Technology, Tokyo. In 2008, he joined NAIST as an assistant professor and has been promoted to associate professor in 2019. His research interests involve bioimaging, biosensing, and electromagnetic field imaging.

Jun Ohta received his ME and Dr. degrees in applied physics from the University of Tokyo, Japan, in 1983 and 1992. In 1983, he joined Mitsubishi Electric Corporation, Japan. In 1998, he joined Nara Institute of Science and Technology (NAIST), Japan, and was appointed as a professor in 2004. His research interests include smart CMOS image sensors for biomedical applications. He is a Fellow of IEEE, the Japan Society of Applied Physics, and ITE.